Effects of Impurity on Void Formation at Interface between Sn-3.0Ag-0.5Cu and Cu Electroplated Film

Ping-Chen Chiang
National Chung Hsing University
Yu-An Shen
Feng Chia University
Chih-Ming Chen (chencm@nchu.edu.tw)
National Chung Hsing University https://orcid.org/0000-0003-4481-1094

Research Article

Keywords: Kirkendall effect, Impurity, Electroplated Cu, EBSD, Solder Joint

Posted Date: February 17th, 2021

DOI: https://doi.org/10.21203/rs.3.rs-230408/v1

Version of Record: A version of this preprint was published at Journal of Materials Science: Materials in Electronics on April 8th, 2021. See the published version at https://doi.org/10.1007/s10854-021-05824-7.

Abstract

Void formation is a critical reliability concern for solder joints in electronic packaging. The control of microstructures and impurity quantities in Cu electroplated films significantly affects the void formation at the joint interface, but the studies for their comparison are seldom. In this study, three Cu films (termed as A, B, and C) are fabricated using an electroplating process. The Cu A film has a facted grain texture embedded with twins while Cu B and C have a similar columnar texture. After thermal aging at 200°C for 1000 h, the SAC 305 (Sn-3.0Ag-0.5Cu) solder joints with Cu A and B exhibit a robust interfacial structure without voids. However, microstructural collapse is observed in the solder joint of SAC 305/Cu C, where many crevives parallel to the interface are formed. Based on the microanalysis, the concentration of impurity is higher in the Cu C film than those in Cu A and B. Moreover, discrete voids rather than continuous crevices are presented in the SAC305/Cu C system when the impurity concentration in Cu C is reduced. The findings demonstrate that the impurity control in the Cu electroplated film is critical for the control of void/crevice formation in the electronic solder joints.

1. Introduction

Electroplating copper (Cu) is an important technology to fabricate the metallizations and conducting traces for signal transmission in electronic devices. One important application is the Sn-rich solder/Cu interconnection in advanced electronic packaging [1, 2]. Functional organic compounds as additives in the plating solutions play a vital role to control the Cu microstructure and property for specific purposes. However, due to strong adsorbability to the Cu electrodeposits the organic additives inevitably co-deposit with the reduced Cu atoms to some extent, leading to the impurity incorporation in the Cu electrodeposits. Excessive incorporation of impure species affects the atomic arrangements and leads to the formation of defects in the Cu electroplated film. Vacancy is one of the most critical defects that can significantly change the material property. For example, vacancy accumulation to form voids at the interface between the Sn-rich solder and Cu film during thermal aging decreases the soldering strength [3, 4].

Some studies have been dedicated to decreasing the level of the impurity incorporation in electroplated Cu to suppress the void formation through the optimization of additive formulation [1, 4, 5]. On the other hand, plenty of studies presented the void formation at the interfaces of solder joints could be suppressed by constructing the Cu microstructures with coherent twin boundary or larger grain size [6–8]. These specific microstructures enabled to block the paths for vacancy accumulation, making voids hardly to nucleate. Although the control of impurity quantity and Cu microstructure can both suppress the void formation at the Sn-rich solder/Cu joints, the studies that take into consideration both factors are rarely seen. Therefore, which factor dominating the void formation is still unclear. In this study, three different Cu films (termed as Cu A, B, and C) were prepared using electroplating, and their impurity quantity and grain microstructure were adjusted by fine-tuning the formulation of organic additives. The Cu A film possessed a similar impurity concentration with Cu B but a different microstructure from Cu B. The Cu C film possessed an impurity concentration much higher than Cu A and B, but its microstructure is similar to that of Cu B. The results of this study revealed that the impurity concentration played a more

significant effect on the void formation at the interface between Sn-3.0Ag-0.5Cu (SAC305) solder and electroplated Cu.

2. Experimental Procedures

Si of 1 cm × 1 cm, with a sputtered Ta layer of 100-nm thick and a sputtered Cu seed layer of 200-nm thick, was used as the substrate for the deposition of Cu electroplated film. An electroplating bath of Cu was constructed using the Ta/Cu-coated Si substrate (cathode), a Cu plate with 0.04 wt.% P (anode), and an electrolyte with high-purity $CuSO_4$, $H_2SO_{4(aq)}$ of 5 vol.%, and proper $H_2O_{2(aq)}$, as shown in Fig. 1. Additionally, different concentrations of an organic additive were added into the plating solution as the key to control the impurity concentration and grain microstructure in the Cu electroplated films. The current density was set as 40 mA/cm^2 for all additive formulation using a power supply (Autolab PGSTAT302N, Netherlands) for 30 min. In this study, three different Cu films were fabricated using the above-mentioned electroplating parameters and the main difference was the additive concentration. Mechanical stirring of 1000 r.p.m was required for uniform deposition of Cu.

Microstructural analysis of each Cu electroplated film was performed by electron backscattered diffraction (EBSD, Oxford, UK), equipping a scanning electron microscope (SEM, JEOL JSM-7800F, Japan), and focus ion beam (FIB, JEOL JIB-4601F, Japan) for grain orientations and cross-sectional ion-beam images with clear contrasts of the grain and twin boundary, respectively. The identification of each impurity (such as carbon, oxygen, and sulfur) in the Cu films and their respective intensities were carried out using a secondary ion mass spectrometer (SIMS, ims 4f, CAMECA, France). Then, the Cu films went through a soldering process at 250°C with an Sn-3.0 wt.% Ag-0.5 wt.% Cu solder (SAC305, Senju Metal Industry Co., Japan). The SAC305 solder was 22 mg and reflowed upon a soldering area of 1.8-mm diameter defined by a heat resistant tape on each Cu film, conducting on a hotplate for 30 s (Fig. 1). Solid-state aging in a furnace at 200°C for 1000 h was performed for the SAC305/Cu solder joints to induce the void formation. Then, the cross-sectional microstructures of the SAC305/Cu interfaces were observed using SEM after grinding and polishing the samples. Energy-dispersive X-ray spectrometer (EDX) equipped to SEM was used to determine the compositions of the reaction products.

3. Results And Discussion

Figure 2 shows the EBSD orientation image map (OIM) of each Cu electroplated film in the normal direction (ND). The color for each grain orientation in the Cu films is represented by an inverse pole figure (IPF) of Cu in Fig. 2c. For example, green in the IPF represents a grain with a high {110} texture. Figure 2a shows the OIM and the IPF with the distribution intensity for each orientation (IPF-DI) in the Cu A film. The Cu A film was clearly {110}-preferred, and that was supported by the high intensity of {110} in its IPF-DI. The ratio of the {110} grains in the OIM was 78.1% by tolerance of 15° between the crystal directions and the axis of ND. The Cu B and Cu C films also possessed {110}-preferred orientations in ND, as shown in their OIMs and IPFs-DI (Figs. 2b and 2c). The ratios of {110} grains in the Cu B and Cu C films were 73.2% and 81.7%, respectively. The ratio of {110} in each Cu film was summarized in Table 1. Hence, the grain

orientations of all Cu films in ND can all be regarded as highly < 110>-oriented, as shown in their OIMs and IPFs-DI.

Table 1
Ratio of the {110}-preferred grain orientation in each Cu film under a tolerance of 15°.

Cu electroplated film	A	B	C
{110} ratio	78.1 %	73.2 %	87.1 %

The grain orientation at a metallic surface plays a significant effect on the surface diffusion. For example, the surface diffusivity is the fastest on the {111} planes in a face-centered cubic crystal because they are the close-packed planes [9, 10]. Based on the theoretical calculation, the diffusivities of Cu on the {111}, {100}, and {110} planes are $9.42 \cdot 10^{-6}$, $1.19 \cdot 10^{-6}$, and $5.98 \cdot 10^{-6}$ cm^2/s, respectively [11]. On the other hand, “Kirkendall effect” is a theory to explain the vacancy diffusion through an interface between two dissimilar solid materials, and “Kirkendall voids” are formed at one side material with a higher diffusivity. This is the reason that void formation frequently appeared at the interface between Sn-based solder and Cu because the diffusion of Cu into Sn is much faster than that of Sn into Cu [3, 6, 12]. Consequently, the control of the Cu surface orientation is very important to investigate the formation of Kirkendall voids at the SAC305/Cu interface. Because the three Cu electroplated films were all {110}-preferred on their surface, the effect of surface diffusivity on the void formation can be ignored in this study. In other words, the effects of microstructure and impurity concentration on the void formation can be sure compared.

Figure 3 shows the cross-sectional FIB images of the Cu A, B, and C films. The grains in Cu A were embedded with a few twin boundaries (Fig. 3a). In Cu B and C, their grains were columnar-shaped as shown in Figs. 3b and c. Therefore, the microstructure of Cu B was similar to that of Cu C, but they were dissimilar to that of Cu A without the columnar grains. Some articles emphasized that the microstructures of the Cu films significantly induced or suppressed the Kirkendall effect [7, 8, 12]. Among them, the smaller grain size in a Cu film provided numerous grain boundaries for Cu fast diffusion into the Sn-rich solder [7, 13], and the grain boundaries between columnar grains were the paths for vacancy aggregation on the Cu surface [8]. They enhanced the Kirkendall effect at the Sn-rich solder/Cu interface unless Cu nanotwin existed in the Cu films [8, 12]. According to the above-mentioned inference, although the Cu A film possessed twin boundary, but the number of twins was much lower than that previously reported capable of suppressing the void formation. The Cu B and C films were with silimar columnar microstructure that enhanced the formation of Kirkendall voids. Therefore, from the microstructural point-of-view the three Cu films all faced high risks of the void formation.

Figure 4 depicts the interfacial reactions of the SAC305 solder with the Cu A, B, and C films during a thermal aging process at 200 °C for 1000 h. Basically, three intermetallic compounds (IMCs) were observed at the SAC305/Cu interface. The layer-type IMCs were identified as the Cu_6Sn_5 and Cu_3Sn phase using EDX which were formed as a result of the interfacial reactions between Sn-rich solder and

Cu. The Ag_3Sn particles embedded at the SAC305/Cu_6Sn_5 interface were precipitates from the SAC305 solder matrix. At the SAC305/Cu A interface (Fig. 4a), a void-free interlayer was observed after the thermal aging, which was similar to that at the SAC305/Cu B interface (Fig. 4b), although the microstructural difference between Cu A and B was significant (Fig. 3a versus 3b). The Cu B film with columnar grains provided several channels for the diffusion of vacancies from the Cu interior toward the film surface. However, voids were not observed at the SAC305/Cu B interface. Conversely, at the SAC305/Cu C interface where the Cu C film possessed a similar microstructure with Cu B, plenty of voids were formed after thermal aging for 1000 h. Kirkendall effect was clearly observed in the SAC305/Cu C system. Moreover, these voids even propagated across the entire SAC305/Cu interface and connected in series to form many crevices (or cracks) parallel to the interface, forming a IMC/crevice alternating structure. Based on the above examinations, it was concluded that the Cu microstructure is not the only essential factor to induce the formation of Kirkendall voids at the interface between SAC305 and Cu.

On the other hand, some impure species originating from the organic substances in the plating solution usually co-deposit in a Cu electroplated film and segregate in the grain boundaries. An increase in the atomic disarrangement due to the impurity incorporation gives rise to plenty of vacancies in the Cu film, and the void formation is induced by the segregation of vacancies during thermal aging. Therefore, the impurities are considered as another possible source of producing the voids in the Cu films [13]. Herein, the incorporation of impurities such as oxygen (O), sulfur (S), and carbon (C) in the Cu A, B, and C films was examined using SIMS as shown in Fig. 5. Obviously, the incorporation levels of O, S, and C were in the same order of Cu C > Cu B ≈ Cu A. In Fig. 4, the SAC305/Cu A and SAC305/Cu B solder joints were void-free. Although the microstructure of Cu B resembled that of Cu C, serious void propagation occurred in the interlayer between SAC305 and Cu C during thermal aging. The results demonstrated that, rather than the microstructures of the Cu films, the impurity level in the Cu films were highly related to the void formation in the SAC305/Cu solder joints thermally aged at 200 °C. The impurities incorporated in the Cu films played the roles to produce plenty of vacancies nucleating at the SAC305/Cu C interface. Segregation of the impure species or their derivatives in the grain boundaries might also annihilate the vacancy sinking sites which accelerated the accumulation of vacancies to form voids [14–16]. Severe void propagation gave rise to the formation of continuous crevices or cracks which was a kind of volumetric defects in crystal caused by void nucleation during annealing [17, 18].

To further investigate the impurity effect, a new Cu electroplated film (termed as Cu C*) was prepared by reducing the additive concentration. The Cu C* film possessed a microstructure similar to that of Cu C but a lower impurity concentration as shown in the SIMS patterns in Fig. 5. Figure 6 shows the cross-sectional SEM image of the SAC305/Cu C* interface after thermal aging at 200 °C for 1000 h. Discrete voids were found but these voids had not propagated and aggregated together to form continuous crevices as those in the SAC305/Cu C system shown in Fig. 4(c) and 4(d). Such different void evolution can be attributed to the level of impurity incorporated in the Cu films. As shown in Fig. 5, the impurity level in the Cu C* film was lower than that of Cu C, so the formation rate of voids caused by the oversaturation of vacancies was lower in the Cu C* film than in Cu C. Therefore, voids were formed discretely instead of

continuous crevices in the SAC305/Cu C* system. In other words, the impurity concentration in the Cu electroplated films plays a crucial role to dominate the void evolution in the form of discrete voids or continuous crevices caused by severe void propagation.

4. Conclusions

Void formation at the interface between solder and Cu is critical for the reliability of solder joints. In this study, the Cu A, Cu B, and Cu C electroplated films all possessed {110}-preferred orientations, identified by EBSD OIM and IPFs-DI, thus the surface diffusion of these Cu films was similar to each other. The microstructural observation of FIB image shows that the Cu B film consisted of numerous columnar grains, which was similar to that of Cu C but was different from that of Cu A with faceted grains embedded with few twin boundaries. After thermal aging at 200 °C for 1000 h, there was no void formation in both the SAC305/Cu A and SAC305/Cu B solder joints although their microstructures were different from each other. Conversely, void formation was observed in the interlayer of the SAC305/Cu C system with a Cu microstructure similar to the Cu B film after thermal aging. Moreover, these voids even propagated inside the IMC layers and connected in series to form crevices (or cracks) periodically inside the IMC layers. Based on the microanalysis of SIMS, the void formation at the solder/Cu interface was rationally explained by the level of impurities incorporated in the Cu electroplated films (Cu C > Cu B ≈ Cu A), rather than their grain microstructures. These results demonstrated the significant effect of impurity on the Kirkendall effect occurring at the interface between SAC305 and Cu film. The findings also suggest that the impurity control of the Cu electroplated film is important for the void suppression in the solder joints of electronic packaging.

Declarations

Conflict of Interest

The authors declare that they have no conflict of interest.

Acknowledgements

The authors acknowledge the financial support of the Ministry of Science and Technology of Taiwan through Grant No. MOST-106-2221-E-005-066-MY3. Chih-Ming Chen thanks the financial support of the “Innovation and Development Center of Sustainable Agriculture” from The Featured Areas Research Center Program within the framework of the Higher Education Sprout Project by the Ministry of Education (MOE) in Taiwan. Yu-An Shen thanks the Ministry of Science and Technology of Taiwan under Project 109-2222-E-035 -008 -MY2.

References

1. H. Lee, Y.A. .Wang, C.M.Chen, Development of nanotwins in electroplated copper and its effect on shear strength of tin/copper joint. J. Alloys Compd. **765**, 335–342 (2018). https://doi.org/10.1016/j.jallcom.2018.06.247
2. Y.-A. Shen, C.Chen, Effect of Sn grain orientation on formation of Cu6Sn5 intermetallic compounds during electromigration. Scr. Mater. **128**, 6–9 (2017). https://doi.org/10.1016/j.scriptamat.2016.09.028
3. F. L.Yin.N. Wafula.P.Borgesen Dimitrov, Toward a better understanding of the effect of cu electroplating process parameters on Cu 3Sn voiding. J. Electron. Mater. **41**, 302–312 (2012). https://doi.org/10.1007/s11664-011-1764-0
4. H. Lee, T.-Y. Yu, H.-K. Cheng, K.-C. Liu, P.-F. Chan, W.-P. Dow, C.-M.Chen, Impurity Incorporation in the Cu Electrodeposit and Its Effects on the Microstructural Evolution of the Sn/Cu Solder Joints. J. Electrochem. Soc. **164**, D457–D462 (2017). https://doi.org/10.1149/2.1171707jes
5. T.-Y. Yu, H. Lee, H.-L. Hsu, W.-P. Dow, H.-K. Cheng, K.-C. Liu, C.-M.Chen, Effects of Cu Electroplating Formulas on the Interfacial Microstructures of Sn/Cu Joints. J. Electrochem. Soc. **163**, D734–D741 (2016). https://doi.org/10.1149/2.0091614jes
6. W.L. Chiu, C.M. Liu, Y.S. .Haung, C.Chen, Formation of nearly void-free Cu3Sn intermetallic joints using nanotwinned Cu metallization. Appl. Phys. Lett. **104**, 171902 (2014). https://doi.org/10.1063/1.4874608
7. P.-F. Chan, H. Lee, S.-I. Wen, M.-C. Hung, C.-M. Chen, W.-P.Dow, Effect of Copper Grain Size on the Interfacial Microstructure of a Sn/Cu Joint, ACS Appl. Electron. Mater. **2**, 464–472 (2020). https://doi.org/10.1021/acsaelm.9b00720
8. P.-C. Chiang, Y.-A. .Shen, S.-P. Feng, C.-M.Chen, Electrodeposition of Twinned Cu with Strong Texture Effect on Voiding Propensity in Electroplated Cu Solder Joints. J. Electrochem. Soc. **167**, 162516 (2021). https://doi.org/10.1149/1945-7111/abd517
9. J.Y. Juang, C.L. Lu, K.J. Chen, C.C.A. .Chen, P.N. Hsu, C.Chen, K.N.Tu, Copper-to-copper direct bonding on highly (111)-oriented nanotwinned copper in no-vacuum ambient. Sci. Rep. **8**, 1–11 (2018). https://doi.org/10.1038/s41598-018-32280-x
10. C.M. Liu, H.W. Lin, Y.S. .Huang, Y.C. .Chu, C. Chen, D.R. Lyu, K.N. Chen, K.N.Tu, Low-temperature direct copper-to-copper bonding enabled by creep on (111) surfaces of nanotwinned Cu. Sci. Rep. **5**, 1–11 (2015). https://doi.org/10.1038/srep09734
11. C.M. Liu, H.W. Lin, Y.C. .Chu, C. Chen, D.R. Lyu, K.N. Chen, K.N.Tu, Low-temperature direct copper-to-copper bonding enabled by creep on highly (1 1 1)-oriented Cu surfaces, Scr. Mater. 78–79 (2014) 65–68. https://doi.org/10.1016/j.scriptamat.2014.01.040
12. H.-Y. Hsiao, C.-M. Liu, H. Lin, T.-C. Liu, C.-L. Lu, Y.-S. Huang, C. Chen, K.N.Tu, Unidirectional Growth of Microbumps on (111)-Oriented and Nanotwinned Copper, Science (80-.). 36 (2012) 1007–1010. https://doi.org/10.1126/science.1216511
13. Z.Zheng, P.-C.Chiang, Y.-T.Huang, W.-T.Wang, P.-C.Li, Y.-H.Tsai, C.-M..Chen, S.-P.Feng, Study of grain size effect of Cu metallization on interfacial microstructures of solder joints, (2019).

https://doi.org/10.1016/j.microrel.2019.05.018

14. Y. Liu, J. Wang, L. Yin, P. Kondos, C. Parks, P. Borgesen, D.W. Henderson, E.J. Cotts, N. Dimitrov, Influence of plating parameters and solution chemistry on the voiding propensity at electroplated copper–solder interface. J. Appl. Electrochem. **38**, 1695–1705 (2008)
15. J.Y. Wu, H. Lee, C.H. Wu, C.F. Lin, W.P. Dow, C.M. Chen, Effects of electroplating additives on the interfacial reactions between Sn and cu electroplated layers. J. Electrochem. Soc. **161**, D522–D527 (2014)
16. H. Lee, S.-T. Tsai, P.-H. Wu, W.-P. Dow, C.-M. Chen, Influence of Additives on Electroplated Copper Films and Their Solder Joints. Mater. Charact. **147**, 57–63 (2019)
17. Y.C. Chu, C. Chen, N. Kao, D.S. Jiang, Effect of Sn grain orientation and strain distribution in 20-μm-diameter microbumps on crack formation under thermal cycling tests. Electron. Mater. Lett. **13**, 457–462 (2017). https://doi.org/10.1007/s13391-017-7041-5
18. S. Liu, T. Song, W. Xiong, L. Liu, Z. Liu, S.Huang, Effects of Ag on the microstructure and shear strength of rapidly solidified Sn–58Bi solder. J. Mater. Sci. Mater. Electron. **30**, 6701–6707 (2019). https://doi.org/10.1007/s10854-019-00981-2

Figures

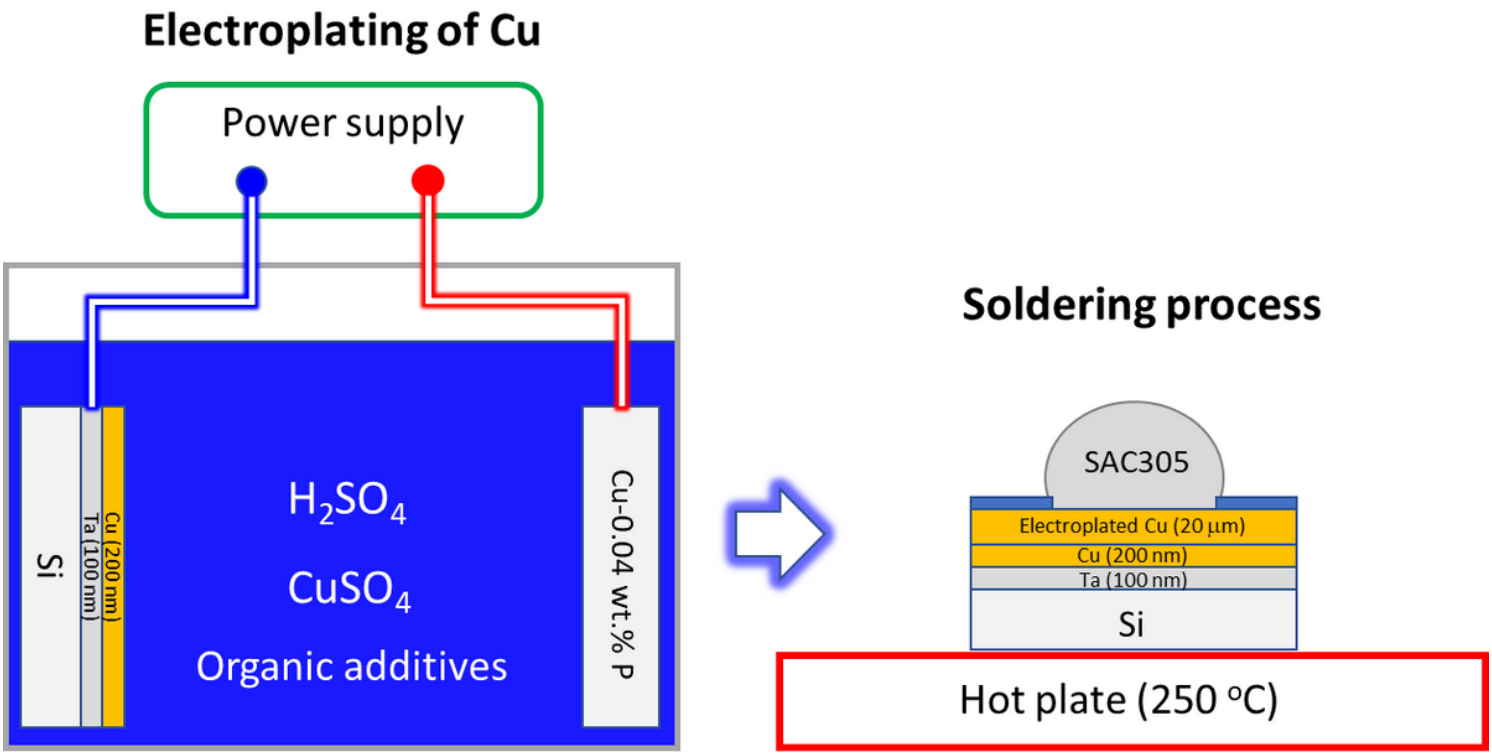

Figure 1

The facility of electroplating Cu and reflow process of SAC305 solder ball on Cu films.

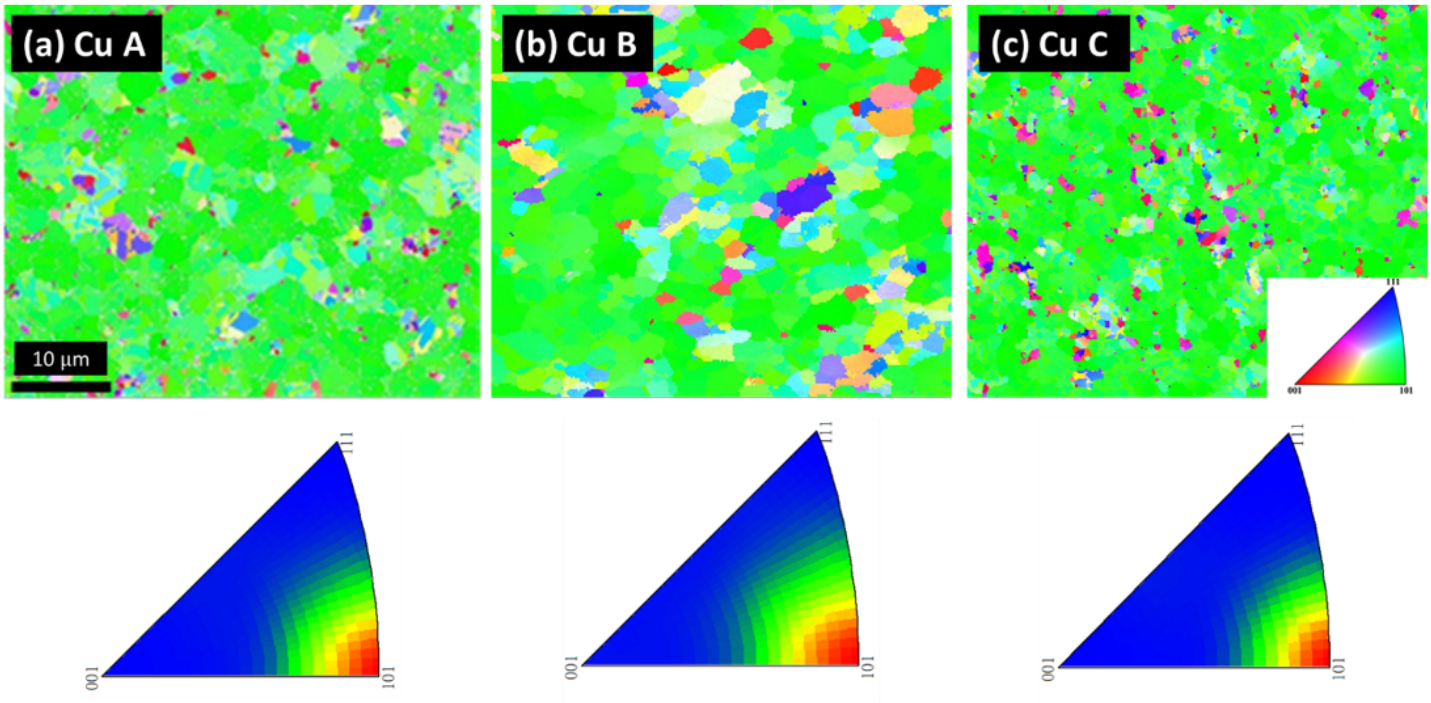

Figure 2

EBSD orientation image maps of the Cu electroplated films and their inverse pole figures with the intensity distriobution of each crystal orientation in the normal direction: (a) Cu A, (b) Cu B, and (c) Cu C.

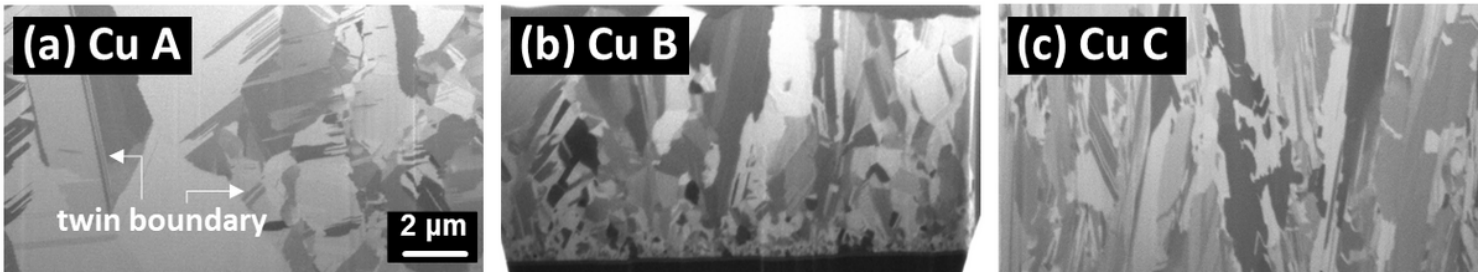

Figure 3

Cross-sectional FIB images of the microstrucutres of the Cu electroplated films: (a) Cu A, (b) Cu B, and (c) Cu C.

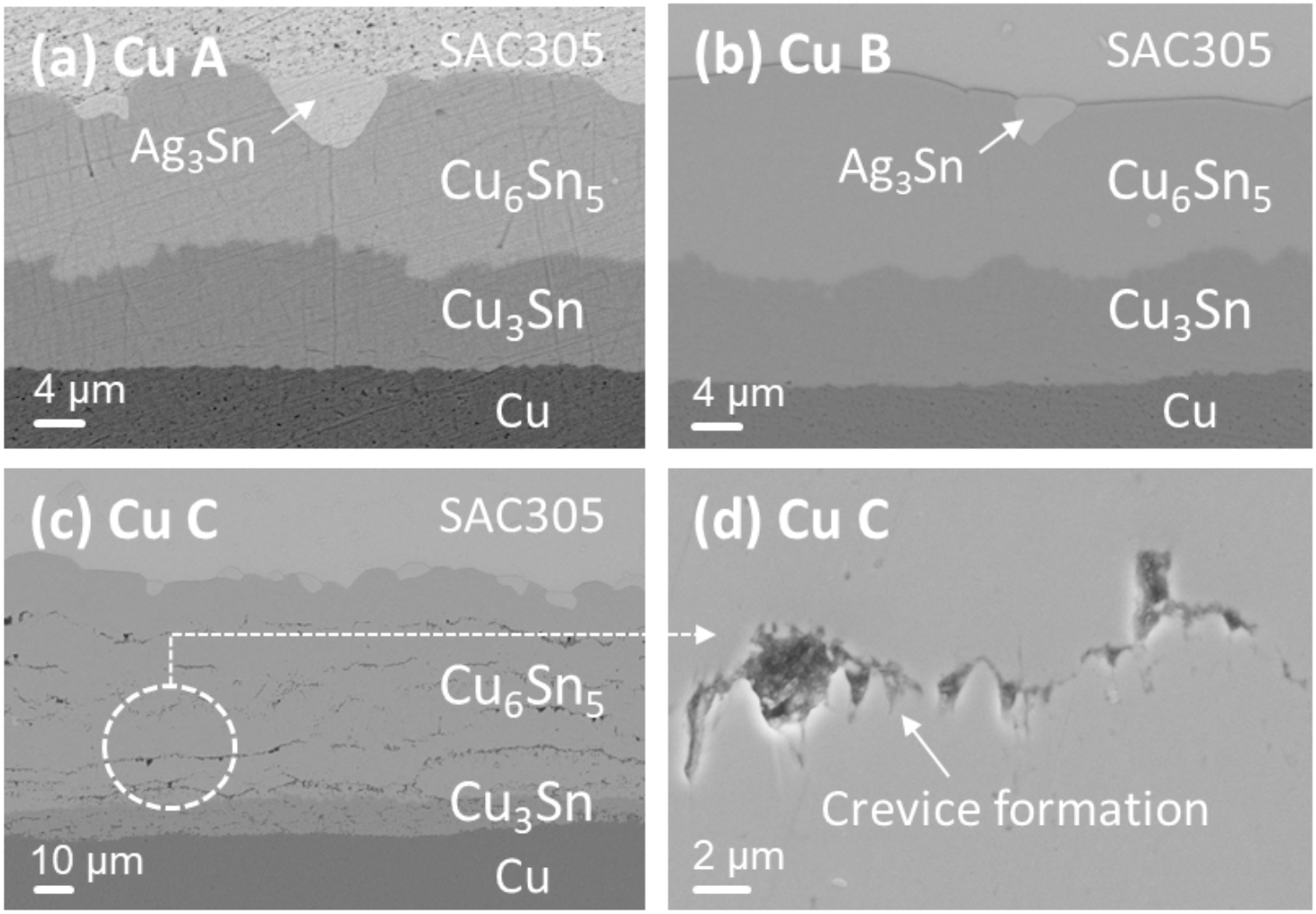

Figure 4

Cross-sectional SEM images of the microstrucutres of the SAC305/Cu interface after thermal aging at 200 ℃ for 1000 h: (a) Cu A, (b) Cu B, and (c) Cu C.

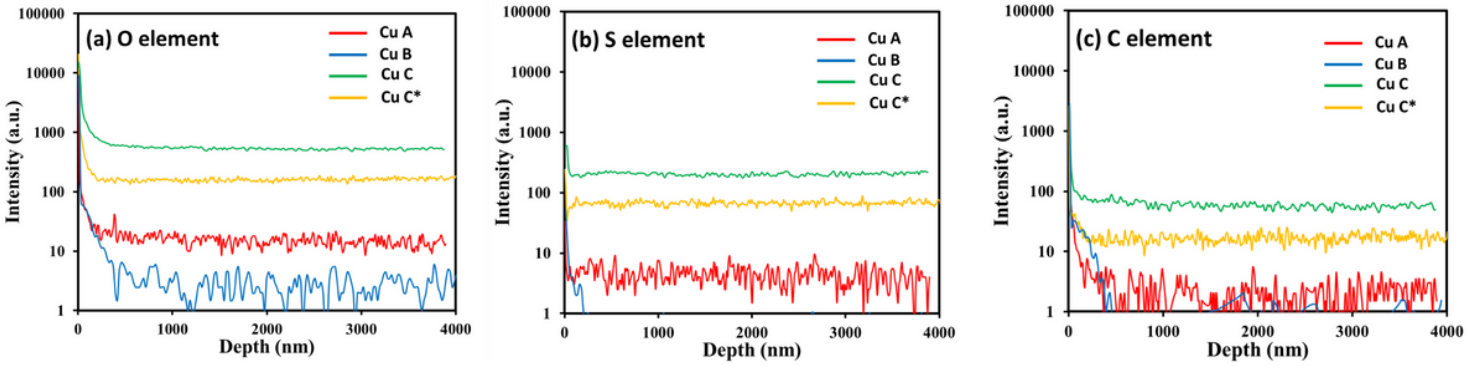

Figure 5

SIMS analyses for O, S, and C intensity in each Cu electroplated film.

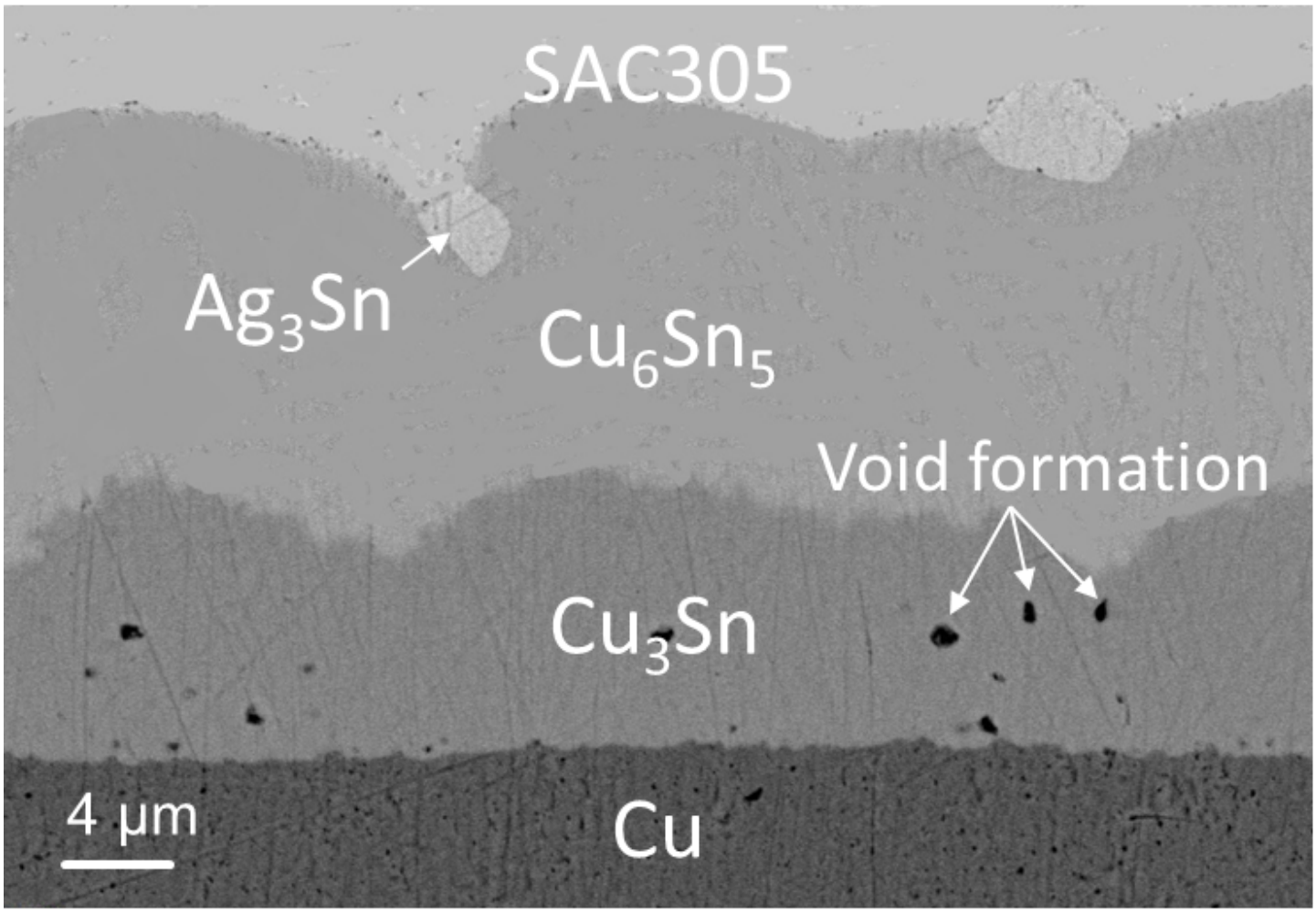

Figure 6

Cross-sectional SEM images of the microstrucutres of the SAC305/Cu interface after thermal aging at 200 °C for 1000 h, where the Cu electroplated film (termed as Cu C*) has a texture similar to Cu C but a lower impurity concentration as shown in Fig. 5.